

Preparative Parameters and Framework Dopant Effects in the Synthesis of Layer-Structure Birnessite by Air Oxidation

Jun Cai,[†] Jia Liu,[†] and Steven L. Suib*,^{†,‡,§}

Departments of Chemistry and Chemical Engineering and Institute of Materials Science, Unit 3060, University of Connecticut, Storrs, Connecticut 06269-3060

Received August 22, 2001. Revised Manuscript Received February 4, 2002

An air oxidation method has been used to synthesize a layer-structure birnessite (OL-1) by the oxidation of Mn^{2+} . The synthesis was accomplished in a much shorter time than other methods such as the reduction of MnO_4^- and redox reactions between Mn^{2+} and MnO_4^- . Thorough investigations of preparative parameters such as the rate and extent of oxidation, the concentration of OH^- , and the aging process were made to understand the synthesis of birnessite using air oxidation. Five metal (Fe, Co, Ni, Ca, and Cd) cations were added to the initial reactant solutions as framework dopants to study their effects on the synthesis and to modify the properties of the resulting birnessite. The crystal phases, average manganese oxidation states, surface areas, and thermal properties of birnessites prepared under different conditions were studied to understand the influence of these conditions on birnessite formation. Birnessite prepared by this air oxidation method was stable up to 500 °C.

Introduction

Layer-structure materials are of great interest because of their potential uses for molecular sieving and catalytic applications.¹ Birnessite (OL-1) is a layer-structure manganese oxide that has edge-sharing MnO_6 octahedra in its layers and metal cations and water molecules in the interlayer region.^{2–6} The distance between layers in birnessite is typically 7 Å. Metal cations can easily move into or out of the interlayer region without significant structural rearrangements because of the hydrated layer-structure nature of birnessite. Therefore, birnessite is a useful and promising material as an ion-exchange material,^{7–9} a cathode material for rechargeable lithium batteries,^{10–12} and

possible heterogeneous catalysts.^{13–16} Birnessite is also an important precursor for the synthesis of tunnel-structure materials. A 6.9 × 6.9 Å tunnel-structure todorokite (OMS-1) can be formed by the hydrothermal treatment of birnessite.^{15,17} A 4.6 × 4.6 Å tunnel-structure cryptomelane (OMS-2) can be produced by the calcination of birnessite.^{18,19}

Synthesis of birnessite can be achieved by the oxidation of Mn^{2+} in basic solutions,^{17–24} by the reduction of MnO_4^- in acidic solutions,^{5,27–29} or by a redox reaction

- * To whom correspondence should be addressed.
- † Department of Chemistry.
- ‡ Department of Chemical Engineering.
- § Institute of Materials Science.
- (1) Mitchell, I. V. *Pillared Layered Structures*; Elsevier Applied Science: New York, 1990.
- (2) Post, J. E.; Veblen, D. R. *Am. Miner.* **1990**, *75*, 477–489.
- (3) Feng, Q.; Yamasaki, N.; Yanagisawa, K. *J. Mater. Sci. Lett.* **1996**, *15*, 963–965.
- (4) Luo, J.; Suib, S. L. *J. Phys. Chem. B* **1997**, *101*, 10403–10413.
- (5) Ching, S.; Petrovay, D. J.; Jorgensen, M. L.; Suib, S. L. *Inorg. Chem.* **1997**, *36*, 883–890.
- (6) Aronson, B. J.; Kinser, A. K.; Passerini, S.; Smyrl, W. H.; Stein, A. *Chem. Mater.* **1999**, *11*, 949–957.
- (7) Nitta, M. *Appl. Catal.* **1984**, *9*, 151–176.
- (8) Golden, D. C.; Dixon, J. B.; Chen, C. C. *Clays Clay Miner.* **1986**, *34*, 511–520.
- (9) Shen, Y. F.; Zerger, R. P.; DeGuzman, R. N.; Suib, S. L.; McCurdy, L.; Potter, D. I.; O'Young, C. L. *J. Chem. Soc., Chem. Commun.* **1992**, 1213–1214.
- (10) Bach, S.; Pereiga-Ramos, J. P.; Baffier, N. *Electrochim. Acta* **1993**, *38*, 1695–1700.
- (11) Bach, S.; Pereiga-Ramos, J. P.; Baffier, N. *J. Solid State Chem.* **1995**, *120*, 70–73.
- (12) Le Cras, F.; Rohs, S.; Anne, M.; Strobel, P. *J. Power Sources* **1995**, *54*, 319–322.

- (13) Matsuo, K.; Nitta, M.; Aomura, K. *J. Catal.* **1978**, *54*, 445–449.
- (14) Jiang, S. P.; Ashton, W. R.; Tseung, A. C. *J. Catal.* **1991**, *131*, 88–94.
- (15) (a) Shen, Y. F.; Suib, S. L.; O'Young, C. L. *J. Catal.* **1996**, *161*, 115–122. (b) Shen, Y. F.; Zerger, R. P.; DeGuzman, R. N.; Suib, S. L.; McCurdy, L.; Potter, D. I.; O'Young, C. L. *Science* **1993**, *260*, 511–515.
- (16) Suib, S. L. *Curr. Opin. Solid State Mater. Sci.* **1998**, *3*, 63–70.
- (17) Golden, D. C.; Chen, C. C.; Dixon, J. B. *Science* **1986**, *231*, 717–719.
- (18) Chen, C. C.; Golden, D. C.; Dixon, J. B. *Clays Clay Miner.* **1986**, *34*, 565–571.
- (19) Cai, J.; Liu, J.; Willis, W. S.; Suib, S. L. *Chem. Mater.* **2001**, *13*, 2413–2422.
- (20) Buser, W.; Graf, P.; Feitknecht, W. *Helv. Chim. Acta* **1954**, *37*, 2322–2333.
- (21) (a) Giovanoli, R.; Staehli, E.; Feitknecht, W. *Chimia* **1969**, *23*, 264–266. (b) Giovanoli, R.; Staehli, E.; Feitknecht, W. *Helv. Chim. Acta* **1970**, *53*, 209–220.
- (22) McKenzie, R. M. *Mineral. Mag.* **1971**, *38*, 493–502.
- (23) Strobel, P.; Charenton, J. C. *Rev. Chim. Miner.* **1986**, *23*, 125–137.
- (24) Yang, D. S.; Wang, M. K. *Chem. Mater.* **2001**, *13*, 2589–2594.
- (25) Liu, L. L.; Feng, Q.; Yanagisawa, K.; Wang, Y. *J. Mater. Sci. Lett.* **2000**, *19*, 2047–2050.
- (26) Golden, D. C.; Chen, C. C.; Dixon, J. B. *Clays Clay Miner.* **1987**, *4*, 271–280.
- (27) Fritsch, S.; Post, J. E.; Suib, S. L.; Navrotsky, A. *Chem. Mater.* **1998**, *10*, 474–479.
- (28) Ching, S.; Roark, J. L.; Duan, N.; Suib, S. L. *Chem. Mater.* **1997**, *9*, 750–754.

between Mn^{2+} and MnO_4^- .^{4,9,17,30} Considerable research has been done on the synthesis of birnessite by reduction and redox methods that involve MnO_4^- . These two methods usually require days and even months for the reaction and aging process to be completed. Work has also been reported on the synthesis of birnessite by oxidation using various oxidizing agents such as O_2 , $S_2O_8^{2-}$, or H_2O_2 . Gaseous oxygen was used in the preparation of birnessite in early work, although there were no systematic studies on synthetic parameters. In this work, air was used to oxidize Mn^{2+} to synthesize birnessite for reasons of cost and ready availability. Preparative parameters that might influence the oxidation of Mn^{2+} , the formation and aging processes, and the properties of birnessite were thoroughly investigated under air oxidation conditions.

Birnessite can be modified for various applications by doping different cations into the layer structure. Physical and chemical properties of birnessite are controlled by the type, amount, and location of the dopants.²³ The doped metal cations can also provide active catalytic sites for different reactions. Framework-doped birnessite can undergo ion exchange and have different types of metal cations in the interlayer region, which can be good precursors to form different tunnel-structure materials. A great deal of work has been done to dope cations into the interlayer region by ion exchange.^{3,4,6,8,22,30} However, few studies have been published using metal cations as framework dopants in the initial reactant solutions, and all of the doping was done by redox reactions between Mn^{2+} and MnO_4^- in the presence of Mg^{2+} that took a few days.^{22,32} Consequently, the reported framework-doped birnessite was actually a mixed doping of magnesium and other metals. In this paper, birnessite has been synthesized by the air oxidation of Mn^{2+} , and various metals have been used as framework dopants added to the original Mn^{2+} solutions. One dopant was added each time to study the unique effect of each doping metal on the synthesis and properties of birnessite. The five different metal ions Fe^{3+} , Co^{2+} , Ni^{2+} , Ca^{2+} , and Cd^{2+} were selected as framework dopants because they can form octahedral metal oxides in the same way as Mn and their hydroxides are not soluble in strong basic solutions. The amounts of metal doping were also varied to study their effects on the syntheses and properties of birnessite.

Experimental Section

Synthesis of Birnessite. In a typical synthesis, a solution of 11.25 g of $MnCl_2 \cdot 4H_2O$ in 75 mL of deionized water was prepared. Air was bubbled into the Mn^{2+} solution at a flow rate of 24 L/min with stirring. A solution containing 30 g of NaOH in 120 mL of deionized water was then added dropwise into the reaction solution. At reaction times of 2, 4, and 6 h, small portions of the products were filtered and washed with water before X-ray diffraction studies were performed to investigate the crystallinity of the products. After 6 h of reaction, the agitation and air bubbling were stopped. The

solution was divided into two parts to study the aging process. One part was kept in solution for 24 h to study the effect of wet aging, and the other part was filtered without washing and air-dried in a funnel for 24 h to study the effect of dry aging. At intervals of 6 h, small amounts of products from both parts were removed and washed to study their crystallinity. The air flow rates and amounts of NaOH were varied in this process. Various metals were doped by adding certain amounts of metal chlorides into the initial Mn^{2+} solutions according to M/Mn atomic ratios of 1/20, 1/10, 1/5, and 1/3. The products were ion-exchanged with KCl solutions and then filtered and washed three times with 1 L of deionized water. The final products were dried in air at 65 °C for 24 h.

Characterization. X-ray diffraction (XRD) was performed on a Scintag XDS 2000 diffractometer with a $Cu K\alpha$ radiation source.

Inductively coupled plasma atomic emission spectroscopy (ICP-AES) analyses were performed on a Perkin-Elmer 7-40 instrument equipped with an autosampler. Dried birnessite powder samples were weighed and dissolved in a 1% HCl solution. Manganese and dopant cations were analyzed. The average oxidation state of manganese in birnessite was determined by a potentiometric titration method.³³

Fourier transform infrared (FTIR) spectra were recorded on a Nicolet Magna-IR System 750 FT-IR spectrometer with an MCT-B detector. The black birnessite powder was diluted with KBr at a ratio of 1:100 and then pressed into a pellet.

Morphology was studied using a Zeiss DSM 982 Gemini field emission scanning electron microscope (FESEM). Specific surface area measurements were done with a Micromeritics ASAP 2010 accelerated surface area and porosimetry system. Nitrogen was used as the adsorbate, and the surface area was calculated using the BET method.

Thermogravimetric analyses (TGA) were performed on a Hi-Res TGA 2950 model thermogravimetric analyzer. The temperature ramp for TGA was 10 °C/min, and the carrier gas was nitrogen.

Temperature-programmed desorption combined with mass spectrometry (TPD-MS) was carried out on a MKS-UTI PPT quadrupole residual MS gas analyzer. A sample of 50 mg of birnessite was purged in He for 4 h and then heated at a rate of 10 °C/min to 700 °C. The downstream gas was analyzed using the MS system.

Results

Synthesis of Birnessite. To understand the factors that affect the synthesis of birnessite, such as the conditions of air flow, the concentration of OH^- , and the effects of aging, preparative parameters associated with these factors were varied in the synthesis.

Time of Air Oxidation. XRD patterns a–c in Figure 1 show the phases of birnessites synthesized at different oxidation times at an air flow rate of 24 L/min. Birnessite had already been formed after 2 h of oxidation of $Mn(OH)_2$. All peaks were due to birnessite except for the one at a 2θ value of 19.5°. This peak was due to feitknechtite (β - $MnOOH$) formed in the process of $Mn(OH)_2$ oxidation. After 4 h of oxidation, the intensities of the birnessite peaks increased significantly, while the intensity of feitknechtite peaks decreased at the same time. The feitknechtite phase disappeared, while the birnessite peaks became more intense when the oxidation time reached 6 h. Birnessite was the only crystallized product after 6 h of air oxidation of $Mn(OH)_2$.

Flow Rate of Air. To study the effect of the rate of oxidation on the formation of birnessite, the flow rate

(29) Luo, J.; Zhang, Q.; Suib, S. L. *Inorg. Chem.* **2000**, *39*, 741–747.

(30) Shen, Y. F.; Suib, S. L.; O'Young, C. L. *J. Am. Chem. Soc.* **1994**, *116*, 11020–11029.

(31) Luo, J.; Zhang, Q.; Huang, A.; Giraldo, O.; Suib, S. L. *Inorg. Chem.* **1999**, *38*, 6106–6113.

(32) Laberty, C.; Suib, S. L.; Navrotsky, A. *Chem. Mater.* **2000**, *12*, 1660–1665.

(33) Xia, G. G.; Tong, W.; Tolentino, E. N.; Duan, N. G.; Brock, S. L.; Wang, J. Y.; Suib, S. L.; Ressler, T. *Chem. Mater.* **2001**, *13*, 1585–1592.

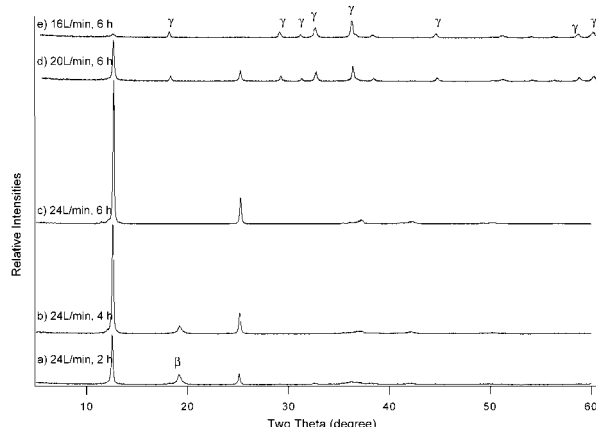


Figure 1. XRD patterns of birnessites prepared at different oxidation times and at different flow rates of air (γ , γ - Mn_2O_3 ; β , β - MnOOH).

of air was varied to change the rate of oxidation. When the flow rate was reduced from the standard value of 24 to 20 or 16 L/min, γ - Mn_2O_3 appeared with birnessite in the oxidation products. Birnessite was still the dominant phase when the flow rate was 20 L/min; γ - Mn_2O_3 became the dominant phase when the flow rate was further reduced to 16 L/min, as shown in Figure 1d and 1e. Prolonged air oxidation did not reduce the intensities of the γ - Mn_2O_3 peaks but did increase the intensities of the birnessite peaks in the XRD patterns. When the air flow was increased to a flow rate higher than 24 L/min, feitknechtite disappeared in a shorter time.

Concentration of OH^- . The concentration of OH^- (C_{OH^-}) was varied by changing the amount of NaOH added. When the amount of NaOH added was the exact amount of NaOH needed to react with Mn^{2+} to form $\text{Mn}(\text{OH})_2$, γ - Mn_2O_3 was the only product, suggesting that Mn^{2+} could not be oxidized to Mn^{4+} at $C_{\text{OH}^-} = 0$. However, if prepared at C_{OH^-} higher than 0.18 mol/L, all of the products formed were birnessite. The average oxidation states of manganese were 3.57, 3.60, 3.58, 3.57, and 3.59 for birnessites prepared with C_{OH^-} values of 0.18, 0.37, 1.3, 2.3, and 3.2 mol/L, respectively. Apparently, at an air flow rate of 24 L/min, birnessite could be synthesized over a wide range of OH^- concentrations without significantly affecting the average oxidation state of manganese.

XRD patterns of birnessites prepared at different OH^- concentrations revealed that birnessite peaks were broad and weak at low OH^- concentrations and became narrower and more intense with increasing concentration of OH^- . Figure 2 shows the sizes of birnessite crystallites prepared at different C_{OH^-} values calculated from the birnessite peak widths using the Scherrer formula.³⁴ The crystal sizes of birnessites increased gradually from 10 to 45 nm when C_{OH^-} was increased from 0.18 to 3.2 mol/L. Morphology studies done by FESEM (Figure 3) also showed that the particle sizes of birnessite became larger with an increase in the concentration of OH^- . The particles seen in FESEM were formed by the aggregation of birnessite crystallites, although the average crystal size of birnessite deter-

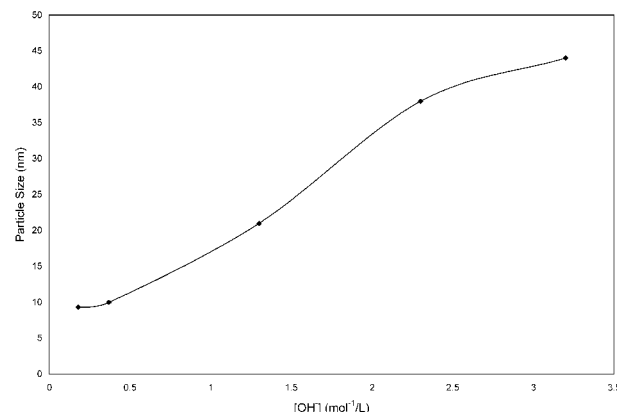


Figure 2. Crystal sizes calculated from XRD peaks of birnessites prepared at different OH^- concentrations.

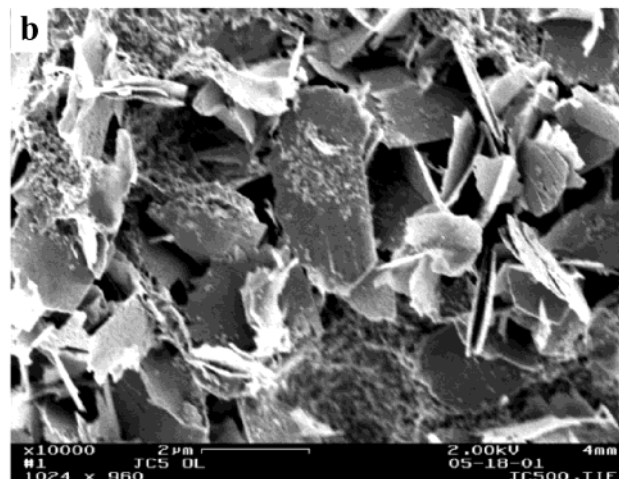
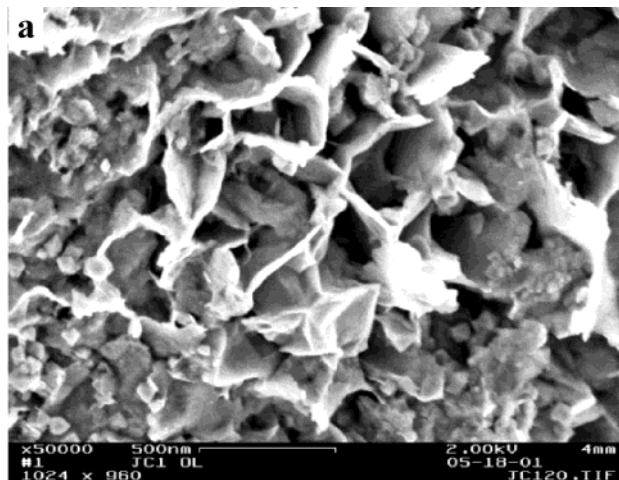


Figure 3. FESEM of birnessites prepared at (a) $C_{\text{OH}^-} = 0.18$ mol/L and (b) $C_{\text{OH}^-} = 3.2$ mol/L.

mined by FESEM was similar to that determined by XRD. Studies on different reaction times at different OH^- concentrations revealed that the reaction time only slightly affected the crystallite and particle size.

Surface area measurements of birnessite prepared at different OH^- concentrations, as shown in Figure 4, revealed that the surface area of the birnessites decreased gradually with increasing concentration of OH^- . The surface area of birnessite decreased from 70 to 30 m^2/g when the OH^- concentration increased from 0.18

(34) Cullity, B. D. *Elements of X-ray Diffraction*, 2nd ed.; Addison-Wesley Publishing Company: Reading, MA, 1978; pp 99–106.

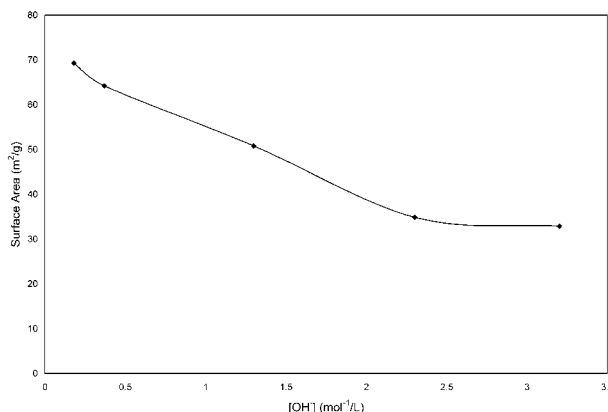


Figure 4. BET surface areas of birnessites prepared at different OH^- concentrations.

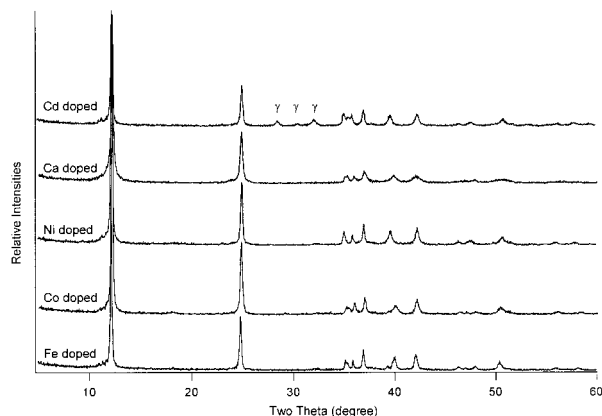


Figure 5. XRD patterns of aged birnessites prepared in the presence of different metal dopants ($\text{M/Mn} = 1/20$) at a flow rate of 24 L/min (γ , $\gamma\text{-Mn}_2\text{O}_3$).

to 3.2 mol/L, confirming that the crystal and particle sizes of birnessites increased along with the concentration of OH^- .

Methods and Time of Aging. Birnessite formed after a typical synthesis ($\text{C}_{\text{OH}^-} = 3.2 \text{ mol/L}$) was aged by two different methods: wet aging and dry aging. In wet aging, birnessite was kept in solution without stirring and bubbling. In dry aging, birnessite was filtered under air but not washed.

Using the wet-aging method, no additional oxygen entered the reaction solution to cause further oxidation. The intensities of the major XRD peaks of birnessite remained basically the same, but minor peaks grew narrower and more intense during the aging time. For example, the peaks of birnessite at 2θ values between 35 and 40° in Figure 1 were better separated after aging, as shown in the XRD patterns of aged birnessites in Figure 5. However, compared with birnessite immediately after 6 h of oxidation, the wet-aged birnessite had one more peak at 19.5° that was due to the feitknechtite phase.

When birnessite was aged under dry conditions and was further oxidized, the XRD patterns showed that the birnessite peaks grew over time and became narrower without the appearance of the feitknechtite phase. Dry aging prevented the formation of feitknechtite that took place in wet aging.

Effects of Metal Doping. Before the studies of the effects of metal doping, synthetic birnessite was ion-exchanged with K^+ to remove Na^+ and any dopant

Table 1. Elemental Compositions of Various Metal-Doped Birnessite Samples As Determined by ICP-AES

| sample dopant/Mn ratio | dopant/Mn ratio ^a determined by ICP-AES | | | | |
|------------------------------|--|-------|-------|-------|-------|
| | Fe/Mn | Co/Mn | Ni/Mn | Ca/Mn | Cd/Mn |
| 1/20 | 0.058 | 0.056 | 0.055 | 0.042 | 0.050 |
| 1/10 | 0.103 | 0.106 | 0.114 | 0.090 | 0.092 |
| 1/5 | 0.212 | 0.199 | 0.227 | 0.195 | 0.200 |
| 1/3 | 0.329 | 0.347 | 0.367 | 0.307 | 0.243 |

^a Ratios shown are molar ratios.

metal (M) cations in the interlayers. The amounts of K^+ analyzed by ICP-AES in all samples were similar, and the $\text{K}/(\text{Mn} + \text{M})$ ratios were around 0.25. Na^+ was completely replaced by K^+ after ion-exchange. To ensure that no cations other than K^+ remained in the interlayers, birnessite samples were program heated to 800 °C to study their thermal transformations, as suggested by Golden et al.⁸ No manganese oxide phase other than cryptomelane was observed, suggesting that only K^+ was present in the interlayer region because the existence of other cations would cause the formation of other manganese oxide phases.⁸

Effects of Different Metals. XRD analyses of birnessites prepared in the presence of metal framework dopants showed that Fe^{3+} , Co^{2+} , and Ni^{2+} have no significant effects on the formation of birnessite at an air flow rate of 24 L/min (Figure 5) but facilitate the formation of birnessite at lower air flow rates. Compared with the undoped birnessites formed at rates of 20 or 16 L/min in which $\gamma\text{-Mn}_2\text{O}_3$ coexisted, no product other than birnessite was formed from the reactant solutions doped with Fe^{3+} , Co^{2+} , and Ni^{2+} cations. On the other hand, Cd^{2+} and Ca^{2+} cations generally impeded the crystallization of birnessite and favored the formation of $\gamma\text{-Mn}_2\text{O}_3$. At a flow rate of 20 or 16 L/min, $\gamma\text{-Mn}_2\text{O}_3$ was always the dominant product. Even at a flow rate of 24 L/min, $\gamma\text{-Mn}_2\text{O}_3$ appeared as a minor phase with birnessite in the Cd^{2+} -doped birnessite (Figure 5).

Effects of Doping Amounts. The amount of metal ion doping also influenced the formation of birnessite using this air oxidation method. Table 1 shows the amounts of different metals doped into the birnessites. The XRD peak intensities decreased and the peak widths increased gradually with increasing amounts of doping. Some neighboring minor XRD peaks of birnessite merged into broader peaks at higher doping amounts. This merging happened at higher doping amounts for Fe^{3+} , Co^{2+} , and Ni^{2+} cation-doped birnessites (at a 1/5 doping ratio) than for Cd^{2+} and Ca^{2+} cation-doped birnessites (at a 1/10 doping ratio). In Cd^{2+} - and Ca^{2+} -doped birnessite with doping ratios of 1/5 or higher, phases other than manganese oxides appeared in the XRD patterns. These impurities were found to be CdCO_3 , $\text{Cd}(\text{OH})_2$, and CaCO_3 .

Infrared Spectroscopy of Doped Birnessites. The IR spectrum of undoped birnessite was a typical spectrum of birnessite.³⁵ The doping of Fe^{3+} , Co^{2+} , and Ni^{2+} cations did not generate new bands but caused broadening and small shifts in the $\text{Mn}-\text{O}$ bands. In the IR spectra of excessively Ca^{2+} - and Cd^{2+} -doped birnessites, new bands associated with CaCO_3 , CdCO_3 , and $\text{Cd}(\text{OH})_2$

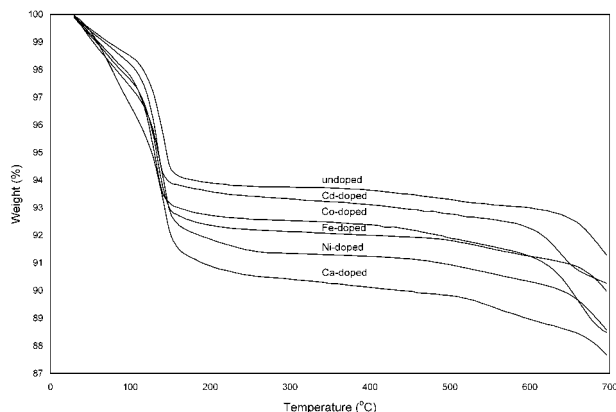


Figure 6. TGA of birnessites prepared in the presence of different metal dopants ($M/Mn = 1/20$) in a nitrogen atmosphere.

Table 2. Weight Losses (%) of Birnessite Samples after Being Heated at 700 °C in Nitrogen As Determined by TGA

| sample dopant/Mn ratio | weight loss (%) determined by TGA | | | | |
|------------------------------|-----------------------------------|-------|-------|-------|-------|
| | Fe/Mn | Co/Mn | Ni/Mn | Ca/Mn | Cd/Mn |
| 0 | 8.71 | 8.71 | 8.71 | 8.71 | 8.71 |
| 1/20 | 10.02 | 11.51 | 11.42 | 12.33 | 9.73 |
| 1/10 | 11.74 | 11.51 | 13.03 | 15.29 | 13.06 |
| 1/5 | 13.41 | 12.10 | 15.74 | 19.34 | 12.25 |
| 1/3 | 14.38 | 13.33 | 17.31 | 18.58 | 11.52 |

appeared along with birnessite bands.³⁶ The IR data confirmed what was revealed in the XRD patterns: that Ca^{2+} and Cd^{2+} could not be incorporated into birnessite as well as Fe^{3+} , Co^{2+} , and Ni^{2+} .

Thermal Analyses. TGA data listed in Table 2 show the weight losses of birnessite samples upon heating at 700 °C in nitrogen. Figure 6 shows typical TGA profiles of metal-doped birnessites. All of the birnessites lost some weight upon heating in a similar process. However, metal doping had a significant impact on the weight lost by birnessite. Weight losses in doped birnessites were larger than those in undoped birnessite. Different metals also had different effects on weight losses. Basically, the weight losses of most birnessites in TGA followed the trend: Ca^{2+} -doped > Ni^{2+} -doped > Fe^{3+} -doped > Co^{2+} -doped > Cd^{2+} -doped > undoped. On the other hand, the weight losses generally increased as the amounts of doping increased, as shown in Table 2.

TPD was used to study the desorption of H_2O , O_2 , and CO_2 from birnessites during heating. In the TPD plot of undoped birnessite (Figure 7), water was lost over a wide range with a peak centered at 200 °C. The loss of framework oxygen species began at about 500 °C. There was a small amount of CO_2 lost during heating. For Fe^{3+} , Co^{2+} , and Ni^{2+} -doped birnessites, all of the losses were similar, except that the water peak was broader and there were a few more small CO_2 peaks. The losses of framework oxygen from Fe^{3+} , Co^{2+} , and Ni^{2+} -doped birnessites started at the same temperature as that for the undoped one. Fe^{3+} , Co^{2+} , and Ni^{2+} doping did not affect the thermal stability of birnessite. However, for Ca^{2+} - and Cd^{2+} -doped birnessites, the loss of frame-

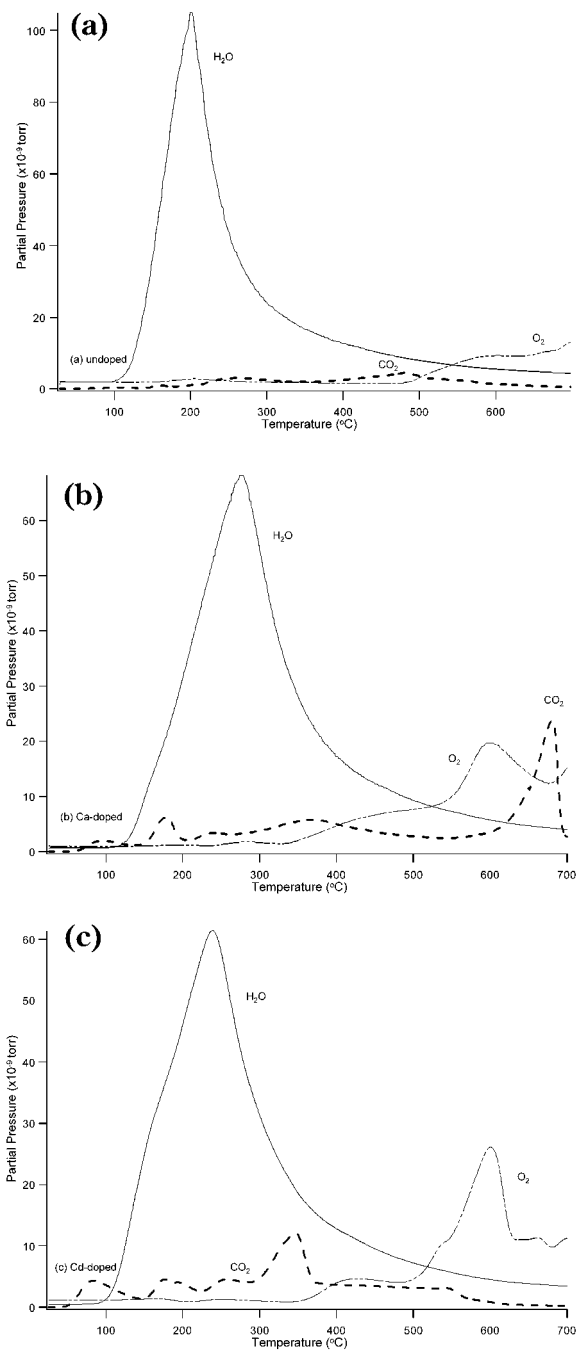


Figure 7. TPD plots of (a) undoped, (b) Ca^{2+} -doped, and (c) Cd^{2+} -doped birnessites in a helium atmosphere.

work oxygen shifted about 100–150 °C to lower temperatures.

Discussion

Because birnessite was prepared by the air oxidation of Mn^{2+} ions in basic solutions, the formation and properties of birnessite were controlled by the following four effects: air oxidation, base concentration, aging, and metal doping.

Effects of Air Oxidation. The flow rate of air was a critical factor in the formation of birnessite. Under the experimental conditions, a flow rate of 24 L/min was essential for the formation of pure-phase birnessite. A lower flow rate produced $\gamma\text{-Mn}_2\text{O}_3$ along with birnessite; the lower the flow rate, the more the $\gamma\text{-Mn}_2\text{O}_3$ in the

(36) Nyquist, R. A.; Kagel, R. O. *Infrared Spectra of Inorganic Compounds*; Academic Press: New York, 1971; pp 216–219.

product. Prolonged oxidation time did not help reduce the amount of $\gamma\text{-Mn}_2\text{O}_3$ after formation. A higher flow rate facilitated the formation of birnessite and reduced the time required to complete the reaction. Therefore, a minimum flow rate of air must be reached to quickly oxidize Mn^{2+} to Mn^{3+} and then to Mn^{4+} . At a low flow rate, the Mn^{3+} formed could not be further oxidized to Mn^{4+} in time to form birnessite, so that $\gamma\text{-Mn}_2\text{O}_3$ was formed instead. Air was unable to oxidize $\gamma\text{-Mn}_2\text{O}_3$ to form birnessite. At high flow rates, Mn^{2+} was quickly oxidized to Mn^{4+} , and birnessite was produced in a shorter time.

In the process of oxidizing $\text{Mn}(\text{OH})_2$ to form birnessite at a flow rate of 24 L/min, $\beta\text{-MnOOH}$ appeared as an intermediate.⁴ The disappearance of $\beta\text{-MnOOH}$ indicated the completion of the conversion of $\beta\text{-MnOOH}$ to birnessite. Using air oxidation, $\beta\text{-MnOOH}$ was completely oxidized to birnessite after 6 h of oxidation, which was much shorter than the 45 days needed for the commonly employed method of oxidizing Mn^{2+} with KMnO_4 in acidic solutions at room temperature.⁴ The time needed to synthesize birnessite was greatly reduced by using this method.

Effects of Base Concentration. Because Mn^{2+} was oxidized in basic solution to form birnessite, the concentration of OH^- was an important parameter in the synthesis and properties of the birnessite. When the amount of OH^- was just sufficient to precipitate Mn^{2+} to form $\text{Mn}(\text{OH})_2$, the basicity of the solution was low. Therefore, the air oxidation of Mn^{2+} was impeded, and $\gamma\text{-Mn}_2\text{O}_3$ was formed. When C_{OH^-} was higher than 0.18 mol/L and the air flow rate was 24 L/min, the oxidation from Mn^{2+} to Mn^{3+} and Mn^{4+} was fast enough that birnessite was formed regardless of C_{OH^-} . The similar average oxidation states of manganese in birnessites prepared at different C_{OH^-} values indicated that air oxidation of Mn^{2+} to form birnessite was complete for $C_{\text{OH}^-} \geq 0.18 \text{ mol/L}$.

The crystal sizes calculated from the XRD peaks and the morphology studies both indicated that the birnessite crystallites increased in size as C_{OH^-} increased. Because increasing reaction time had little effect on increasing the crystal size, C_{OH^-} was the major factor affecting the crystal size of birnessite. MnO_x is an amphoteric oxide, and its solubility increases as C_{OH^-} increases. The large amounts of free MnO_6 units in the reactant solutions with higher C_{OH^-} values might help bring small birnessite crystallites together to form bigger crystallites through the aggregation of MnO_6 units between small crystallites. The decrease in surface area of birnessites with increasing concentration of OH^- also reflected the increase in the birnessite crystal size.

Effects of Aging Process. Aging of the birnessite formed could help the continuous growth and stabilization of the birnessite layer structure. Wet aging and dry aging had different effects on birnessite formation. The feitknechtite phase reappeared after 6 h of wet aging and remained in the products. Because it was possible that some Mn^{2+} and Mn^{3+} ions might have been incorporated into the birnessite formed, Mn^{2+} could have been oxidized by leftover oxygen, and Mn^{3+} could have been hydrated with water and reacted with OH^- to form $\beta\text{-MnOOH}$. $\beta\text{-MnOOH}$ was not further oxidized to form birnessite without an adequate supply of oxygen.

Birnessite had a better structural ordering but did not grow in amount or in crystal size after wet aging, as indicated by the better separation of minor XRD peaks and only minor changes in the intensities and widths of the major peaks. The redissolution and recondensation of some MnO_6 units from birnessite crystallites might give the birnessite higher structural order.

In dry aging, products were in basic environments and were able to be further oxidized by air. Any Mn^{2+} incorporated in the products was quickly oxidized to form birnessite. The possible hydration of Mn^{3+} incorporated into the products could not take place because of a deficiency of water. Therefore, no $\beta\text{-MnOOH}$ was formed during dry aging. At the same time, birnessite lost extra interlayer water to form a better arrangement of MnO_6 layers. This explains why the crystallinity of birnessite kept growing without the formation of $\beta\text{-MnOOH}$ during dry aging. Therefore, dry aging is a better way to age than wet aging for the growth of crystalline birnessite.

Effects of Metal Doping. From the influences of metal doping on both the syntheses and properties of birnessite, Fe^{3+} , Co^{2+} , and Ni^{2+} cations appeared to be better framework dopants than Ca^{2+} and Cd^{2+} cations. Fe^{3+} , Co^{2+} , and Ni^{2+} cations not only facilitated the formation of birnessite at low air flow rates and could be doped into birnessite without producing extra phases in larger amounts, but they also retained the thermal stability of birnessite. Ca^{2+} and Cd^{2+} generally impeded the syntheses and deteriorated the thermal stability of the birnessite.

The different impacts of these two groups of metals on the syntheses and properties of birnessite might be due to their different physical and chemical properties. Fe^{3+} , Co^{2+} , and Ni^{2+} cations have sizes similar to those of $\text{Mn}^{3+/4+}$ cations, whereas Ca^{2+} and Cd^{2+} cations are much larger in size.³⁷ Similar cation sizes allow MnO_6 layers of birnessite to accommodate larger amounts of doping and maintain the integrity of layer structure at the same time. The size differences also explain why Fe^{3+} , Co^{2+} , and Ni^{2+} -doped birnessites were as thermally stable as undoped birnessite, whereas Ca^{2+} - and Cd^{2+} -doped birnessites were less thermally stable. Large Ca^{2+} and Cd^{2+} cations produced high stress and caused the breakdown of the birnessite layer structure at low temperatures. The different chemical properties of these metals might account for their different effects on the synthesis of birnessite. The multiple valences of iron, cobalt, and nickel cations might facilitate the oxidation of Mn^{2+} by switching among different valences, especially when the air flow rate is low. Calcium and cadmium cations are monovalent, and their sizes are large compared to those of the manganese cations. Therefore, Ca^{2+} and Cd^{2+} doping impedes the synthesis of birnessites.

Conclusions

Thermally stable layer-structure birnessite has been synthesized and modified by framework metal dopants using an air oxidation method. A minimum flow rate of air is required to oxidize Mn^{2+} in basic solution to

(37) Lide, D. R. *CRC Handbook of Chemistry and Physics*, 73rd ed.; CRC Press: Boca Raton, FL, 1992; p 12-8.

synthesize birnessite without the formation of γ -Mn₂O₃. Birnessite was synthesized in a much shorter time by this method as compared to other methods. An OH⁻ concentration of 0.18 mol/L is essential to form birnessite, and higher OH⁻ concentrations increase the crystal size but decrease the surface area of the birnessite. Dry aging is a better way to form well-ordered birnessite than wet aging. Fe³⁺, Co²⁺, and Ni²⁺ doping facilitates the formation of birnessite and retains its thermal stability, whereas Ca²⁺ and Cd²⁺ doping impedes the

formation of the birnessite and deteriorates its thermal stability.

Acknowledgment. We acknowledge support from the Geosciences and Bioscience Division, Office of Basic Energy Sciences, Office of Science, U. S. Department of Energy. We also thank Dr. Francis S. Galasso for helpful discussions.

CM010771H